Environmental Science & Technology

Article

Cite This: Environ. Sci. Technol. 2018, 52, 11132−11141

pubs.acs.org/est

Real-Time Study of Rapid Spread of Antibiotic Resistance Plasmid in Biofilm Using Microfluidics

Bing Li,[†,‡,§] Yong Qiu,[*,‡] Jing Zhang,[‡] Xia Huang,[‡] Hanchang Shi,[‡] and Huabing Yin[*,§]

[†]School of Energy and Environmental Engineering, University of Science and Technology Beijing, Beijing, 100083, China

[‡]State Key Joint Laboratory of Environment Simulation and Pollution Control, School of Environment, Tsinghua University, Beijing 100084, P. R. China

[§]Division of Biomedical Engineering, School of Engineering, University of Glasgow, Glasgow, G12 8LT, U.K.

Supporting Information

ABSTRACT: Gene transfer in biofilms is known to play an important role in antibiotic resistance dissemination. However, the process remains poorly understood. In this study, microfluidics with time-lapse imaging was used for real-time monitoring of plasmid-mediated horizontal gene transfer (HGT) in biofilms. *Pseudomonas putida* KT2440 harboring an antibiotic resistance plasmid RP4 was chosen as the donor while *Escherichia coli* and activated sludge bacteria were used as the recipient cells. Dynamic features of the transfer process, including the transfer rate, cell growth rate and kinetic changes of the transfer frequency, were determined. It was found that the routes for gene transfer strongly depend on the structure and composition of a biofilm. While intraspecies HGT is essential to initiate a transfer event, the secondary retransfer from transconjugants to the same species is more efficient and can cause cascading gene spread in single-strain biofilms. For the activated sludge biofilm, only small and scattered colonies formed and vertical gene transfer appears to be the dominant route after initial intraspecies transfer. Furthermore, more than 46% of genera in the activated sludge were permissive to plasmid RP4, many of which are associated with human pathogens. These phenomena imply early prevention and interruptions to biofilm structure could provide an effect way to inhibit rapid antibiotic resistance gene spread and reduce the likelihood of catastrophic events associated with antibiotic resistance.

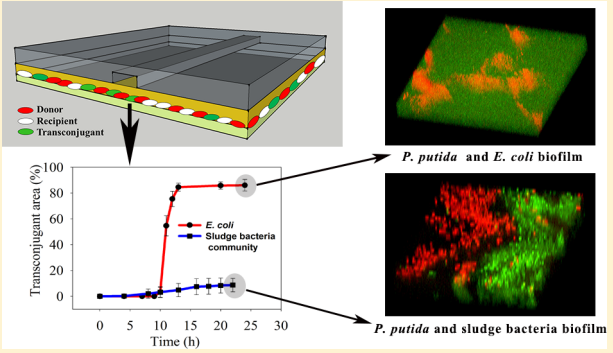

INTRODUCTION

The rapid spread of antibiotic resistance has become a global crisis and imposes significant threats to human health and the natural environment. Although bacteria live either as planktonic cells or in biofilms,[1] ∼80% of human bacterial infections have been found to be biofilm-related.[2] An in-depth understanding of how antibiotic resistance spreads in biofilms is therefore pivotal to tackle this crisis.

Horizontal gene transfer (HGT) is a widely recognized mechanism for adaptation in bacteria.[3] HGT consists of three main routes: plasmid-mediated conjugation, transduction and transformation. Plasmid-mediated conjugation can transfer DNA between genera and phyla.[4] Because of dense cell populations, conjugation in biofilms is generally high,[5] and was considered as a major pathway for spreading antibiotic resistance genes (ARG). ARG dissemination not only contributes to the resistance of biofilms to antimicrobials[6] but also enhances the evolution of ARGs.[7,8] At the individual cell level, it has been shown that conjugation is a dynamic process occurring between cells of the same species (e.g., *Escherichia coli*[9] and *Pseudomonas putida*[10]). However, information about dynamic gene transfer in biofilms is scarce.[4] Little is known about when the transfer occurs and how it propagates within a biofilm, in particular in biofilms of complex communities.

Currently, the study of plasmid transfer in biofilms mainly relies on filter-mating,[11,12] flasks or plate culture.[13,14] These methods can provide a global view of transfer efficiency in biofilms, but do not allow the observation of real-time changes in the community. In recent years, microfluidic technology has opened up a new avenue for applications in microbiology. Manipulation of bacteria at the single-cell level has become well established, leading to the discovery of a variety of new phenomena.[15−18] Similarly, real-time imaging of in situ formation of biofilms on chip has also been demonstrated.[19,20] These evidence suggest that microfluidics can provide a promising platform to investigate the dynamic process of ARG transfer within biofilms.

Here, we employed a microfluidic device for real-time monitoring of gene transfer via plasmid-mediated conjugation in biofilms. We have previously demonstrated that such a

Received: June 15, 2018
Revised: August 20, 2018
Accepted: September 4, 2018
Published: September 4, 2018

device enables precise control of cell microenvironments and the determination of cell growth characteristics with single-cell resolution.[21] In this study, *Pseudomonas putida* (*P. putida*) KT2440 harboring the ARG-encoding plasmid RP4 were used as the donor cells. *Escherichia coli* (*E. coli*) and a mixed microbial community from activated sludge were used as the recipient cells. The plasmid transfer processes between the *P. putida* donor cells and the recipient cells were imaged throughout the course of biofilm formation. Dynamic transfer rate, cell growth rates and the transfer frequency were quantified, which reveal key mechanisms of the gene transfer processes. Furthermore, the genera of the isolated transconjugant pools from the activated sludge communities were determined to identify which members of the community received the ARG-encoding plasmid.

MATERIALS AND METHODS

Bacterial Strains and Culture. The donor strain, *P. putida* KT2440, was a generous gift from Professor Barth F. Smets in Technical University of Denmark.[22] The strain hosts a GFP-encoded Inc.P-1α plasmid RP4 conferring resistance to kanamycin, ampicillin and tetracycline, and is also chromosomally tagged with a red fluorescence gene (*dsRed*) and *lacI*^{q} that represses the expression of GFP.[22] As a result, the donor cells only emit red fluorescence. The recipient cells are nonfluorescent but emit green fluorescence after taking in the GFP-encoded plasmid RP4 (i.e., becoming transconjugants). The amplification of *P. putida* KT2440 strain was carried out in liquid LB broth at 30 °C overnight with the addition of 50 mg·L^{-1} kanamycin as antibiotic stress.

A pure strain of *E. coli* (ATCC 25922, USA) and the bacterial communities extracted from activated sludge were used as the recipient cells. The *E. coli* strain was cultured in LB broth at 37 °C overnight, and harvested by centrifugation prior to the microfluidic experiments. Activated sludge communities were obtained from the wastewater treatment plants (WWTPs) in Wuxi, China. The activated sludge sample was first mashed in a high-speed tissue mill (Bilon JJ-2, Shanghai Bilon Company, China) for 1 h to extract bacteria cells from the floc aggregation. During this process, the sample was crushed for 5 min in every 10 min. The mixed liquor from this pretreatment was cultured on R2A medium at 30 °C overnight and then harvested as the mixed bacterial community. This selects growing bacteria from the community but removes noncultivable species.

Mating Assays within a Microfluidic Chip. The microfluidic device was fabricated as described previously.[15] In brief, the device consists of four components: a coverslip, a thin layer of agarose membrane, a PDMS chip, and a manifold (Supporting Information (SI) Figure S1). The PDMS chip contains a single channel with 13 mm length, 500 μm width, and 500 μm depth, flowing broth continuously for bacterial growth. The nutrients in the flow diffuse through the agarose membrane into the bacterial layer, and at the same time, the metabolic waste diffuses out of the membrane and is carried away by the flow. The agarose membrane is 250 μm thick and made from 2% agarose (Sigma-Aldrich) in RO water. This on-chip culture enables rapid exchange of substances and allows high density growth, and thus provides a close-to-in vivo model to study real-world biofilms.[23]

The donor and recipient cells were first washed with PBS (three times) and then diluted in LB or R2A medium to a concentration of ~10^8 cells·mL^{-1}. They were then mixed at a ratio of 1:1 for on chip experiments. A drop of 5 μL mixed bacterial solution was sandwiched between the coverslip and the agarose membrane, prior to assembling of the four components. On a control chip, 5 μL of the recipient cells were inoculated at the same time. LB or R2A medium was continuously delivered into the microchannel at a flow rate of 2 μL·min^{-1} to provide a constant supply of the nutrients and remove the waste. No transfer events were detected if only PBS was used (SI Figure S2). Each mating assay lasted for 24 h.

Fluorescence Imaging. Time-lapse imaging of the on-chip mating experiments was carried out on an inverted microscope (Ti-E, Nikon Corp., Japan) equipped with a 20× /NA0.45 objective lens and a CCD camera (CCD, iXon X3 897, Andor Company, UK). Bright field and fluorescence images at selected eight to ten zones under and around the microchannel on chip were taken at defined time intervals (e.g., every 5 min or every 1 h). Each imaging site was directly below the microchannel, where the nutrient supply and biofilm thickness were consistent. Since conjugation occurred randomly, >20 repeated experiments were carried out in order to observe statistically meaningful transfer events. GFP fluorescence was detected using excitation of 488 ± 20 nm and emission of 525 ± 40 nm, whereas *dsRed*-based fluorescence was detected using excitation of 561 ± 25 and emission of 650 ± 60 nm. All images were processed with ImageJ as described previously to calculate the number and the area of cell colonies.[15]

At the end of the experiments, the biofilms were further characterized with a laser scanning confocal microscope (LCSM, LSM710, Zeiss, German). A large area of 12 × 3.5 mm^2 (~21% of the total horizontal cross-section 196 mm^2) was scanned using a 10 × /NA0.45 objective lens. For the areas containing transfer events, high-resolution images were further taken using a 100 × /NA1.40 oil objective lens. Z-scanning with a 2 μm interval was carried out to characterize the internal structure of the biofilms. A uniform thickness of ~18 μm was observed for the biofilms (SI Figure S3).

Calculation of the Transfer Rate and the Transfer Frequency. The dynamics of transconjugant formation is critical to understand the mechanisms of the gene transfer processes. To image a relatively large area, a 20 × /NA0.45 objective lens was used for all time-lapse imaging. The depth-of-field of this lens is 4.27 μm. This defines the detection region in z-length to be ~4 μm from the bottom focal plane, which is within the ~18 μm thickness of the biofilms. Therefore, the areas occupied by transconjugants within an image can be used to calculate their abundance in the biofilm. The transfer rate (R_T) can be derived from the changes of the transconjugant area (A_T%) with time (see the Result section). The A_T% is calculated based on eq 1.

$$A_T\% = \frac{A_T(t)}{A_{total}} \times 100\% \quad (1)$$

where $A_T(t)$ is the green fluorescence area (i.e., the transconjugant area) in a series of time-lapse images at a given time t, A_{total} is the total area of an image, which has a constant value of 0.168 mm^2.

The end-point transfer frequency, defined as the ratio of transconjugants to recipients (T/R), is often used to evaluate transfer efficiencies of plasmids in different settings.[11,12] However, transconjugants can come from several routes, including primary conjugation by the original donors, the

DOI: 10.1021/acs.est.8b03281
Environ. Sci. Technol. 2018, 52, 11132−11141

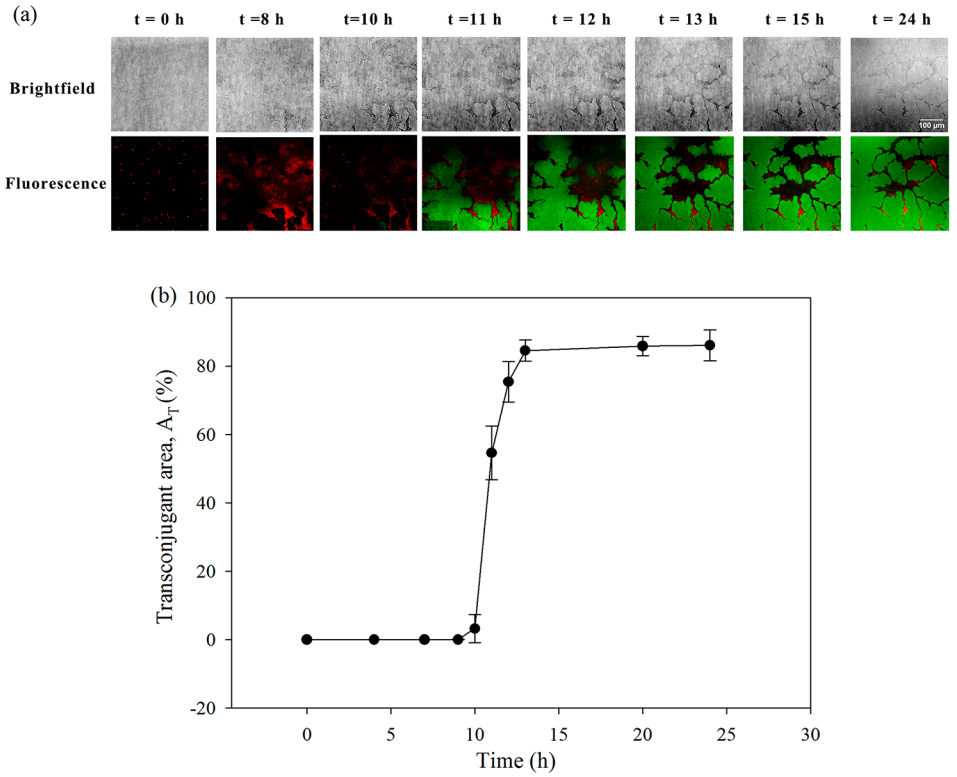

Figure 1. Process of plasmid transfer between *P. putida* KT2440 and *E. coli*: (a) Time-lapse images of both bacteria on chip. *P. putida* KT2440 cells emit red fluorescence. *E. coli* cells are colorless, while *E. coli* transconjugants emit green fluorescence. (b) The changes of the transconjugant area within an image (A_T%) with time (n = 8, the error bars are SD).

secondary conjugation by transconjugants, and by cell division. In the microfluidic device used in this study, cells have fixed locations on chip, and thus the transfer processes can be tracked by time-lapse imaging. This facilitates the identification of the mechanisms involved. In a similar manner to the calculation of A_T%, the localized transfer frequency (F) at selected zones can be determined at a given time according to eq 2.

$$F = \frac{A_T}{A_R} \quad (2)$$

where A_T and A_R are the area of the green transconjugants and the recipient cells within an image at a given time, respectively. The total area of each image is 0.168 mm^2. Only images containing transfer events were used for calculation.

Cell Sorting and Diversity Analysis of the Sludge Biofilms. The activated sludge biofilms were collected after the on-chip mating assay for fluorescence activated cell sorting (FACS) and subsequent 16S rDNA sequencing. To do this, the microfluidic chip was dissembled to allow collection of the detached thin biofilms into a centrifuge tube. The surfaces of the coverslip and agarose gel that were in contact with the biofilm were also washed with 1 mL PBS. Both collections were combined and diluted with PBS to the required concentration of ~10^8 cells·mL^{-1} for FACS (Aria SORP, BD Company). Green fluorescence was excited with a 488 nm laser and the red one with a 561 nm laser. The forward scatter voltage was set at 637 V and the side scatter voltage at 198 V. The gates were set to collect GFP-expressing transconjugants. Activated sludge without the donor cells were used as control. The collected transconjugants and the control were sent to a commercial company (Majorbio, Shanghai, China) for 16S rDNA sequencing (HiSeq PE250 platform, Illunima). Sequence analysis was carried out using the software platform developed by the company (www.i-sanger.com). The protocol is included in the SI.

RESULTS

Cascading Plasmid Transfer in *E. coli* Biofilm. *P. putida* KT2440 donor and *E. coli* recipient cells were used as a model system to study the transfer of the broad-host-range plasmid RP4 in a single-strain recipient biofilm. Figure 1a shows representative time-lapse images of the transfer process from the initial cell seeding. At t = 0 h, individual donor and recipient cells were distributed randomly on the surface. Because of continuous delivery of LB broth on chip (i.e., akin to chemostat culture), exponential growth of cells was maintained.[15] By t = 8 h, the surface was almost fully occupied with cells, where *P. putida* colonies (red) were in contact with *E. coli* cells (colorless) (Figure 1a). By t = 10 h, a thick bacterial biofilm had formed. At this point, a few *E. coli* colonies presented with green fluorescence (Figure 1a), indicating the occurrence of conjugation and successful GFP-expression in the *E. coli* transconjugants. It should be noted that *E. coli* grew faster than *P. putida* KT2440 on chip (SI Figure S4), and thus the areas of *E. coli* transconjugants in the image were larger than that of the *P. putida* KT2440 (Figure 1). As a consequence, the total red fluorescence area appeared to slightly shrink with time (Figure 1a, and SI Figure S5a). Moreover, Z-stack confocal images of the biofilm showed the same distribution of the green and red areas along the z-axis (Figure 2), indicating that the transfer existed across all layers of the biofilm.

DOI: 10.1021/acs.est.8b03281
Environ. Sci. Technol. 2018, 52, 11132−11141

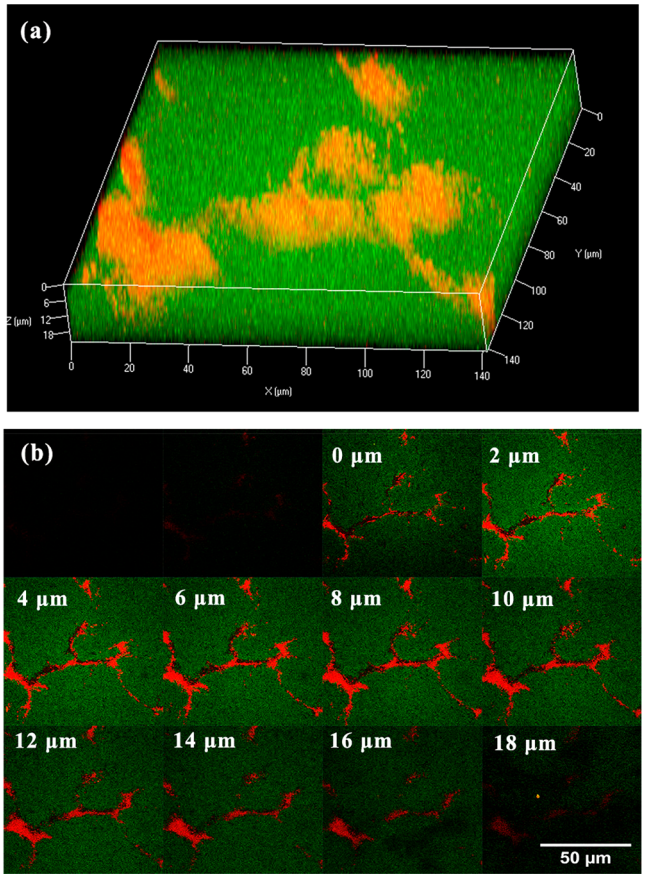

Figure 2. Spatial distribution of transconjugants in the *E. coli.* biofilm with donor *P. putida* KT2440 at 24 h. (a) image of 3-D structure of the biofilm; (b) Z-stack images of different layers at a 2 μm interval. Donor cells emit red fluorescence and transconjugants emit green fluorescence.

Interestingly, after t = 10 h, the transconjugant areas spread rapidly across the biofilm. Plotting the changes of transconjugant areas (A_T%) with time showed a sharp increase from 3.4% at t = 10 h to ~80% at t = 13h (Figure 1b). To study this process in detail, time-lapse images were taken every 5 min between t = 10 h and t = 11 h. Within the first 25 min, a steep increase of the transconjugant areas with time was observed (Figure 3a &b). By fitting the curve with the Michaelis–Menten model, it was found that the transfer rate (R_T) was 1.34%·min^{-1} (or 81%·h^{-1}), indicating a 10-fold increase of the transconjugant areas within the first 25 min (i.e., from 3.4% to 36% in Figure 3b). However, after 25 min, the increase was reduced significantly and eventually the transconjugant areas approached a plateau at ~180 min. This saturation was likely due to the high cell density and hence limited cell growth at this time point—it has been shown that nongrowing recipient cells have substantially reduced conjugal activity.[10]

Although the presence of transconjugants provided convincing evidence of the gene transfer from the *P. putida* donor to the *E. coli* recipient cells, the observed cascading growth of transconjugants (Figures 1 and 3) also raised a question about contributions from other transfer routes, including cell division. To investigate this, the maximum specific growth rates (μ_m) of the *E. coli* cultured on chip were determined as previous described[15] and found to be ~0.89 h^{-1} (SI Figure S4). At this growth rate, cell doubling would require at least 46 min, suggesting cell division alone cannot account for the 10-fold increase of transconjugants within the first 25 min. For the increment stage (t = 10–13 h), the specific increment rate (μ_T) of transconjugants was 2.9 ± 0.89 h^{-1}, obviously higher than μ_m (Table 1). Furthermore, the majority of transconjugants located in the center of *E. coli* growth areas (Figure 1a & 3a), suggesting the secondary conjugation between *E. coli* transconjugants and the same species recipient cells was the dominant driver for the observed cascading gene transfer.

Gene Transfer in Environmental Community Biofilms. Activated sludge contains abundant antibiotic resistance plasmids[24−26] and it is well recognized as a pool for the evolution of antibiotic resistant genes.[27,28] Transfer of the plasmid RP4 from the *P. putida* KT2440 donor cells to the activated sludge community was studied on chip in the same manner as the *P. putida* KT2440 − *E. coli* pair. Similar to the *E. coli* biofilm, at t = 5 h, a dense monolayer of cells was formed on chip, and at t = 8 h the green fluorescence of transconjugants was detected (Figure 4a). However, after that, the transconjugant areas increased gradually and continuously until the end of the experiments. It is worth noting that all the observed conjugation events occurred randomly within the sludge bacterial community biofilm and showed the same features as *E. coli* biofilm (SI Figure S5b).

Interestingly, the curve of the transconjugant area (i.e., A_T%) versus time for the activated sludge biofilm exhibits typical characteristics of a bacterial growth curve, including lag-, exponential-, stationary-, and declined phases (Figure 4b). Thus, the exponential growth model is suitable for data interpretation instead of the Michaelis–Menten model that assumes HGT saturation due to limited recipients. Fitting the "exponential phase" (from 8 to 18 h) of the A_T%-*time* curves with the growth model gives the specific increment rate of transconjugants (μ_T), which is 0.26 ± 0.14 h^{-1} on average based on five randomly selected transconjugant areas (Table 1). This value is lower than the initial average μ_m of the activated sludge community (0.71 h^{-1}) on chip (i.e., as a monolayer) (SI Figure S4). This suggests that cells of slower growth rates tend to be more permissive to the plasmid RP4 and cell division does play an important role for continuous gene dissemination in the sludge community biofilm.

Comparison of Transfer Frequency in Two Biofilms. With time-lapse imaging, dynamic changes of the transfer frequency around the conjugation locations (i.e., localized transfer frequency) can be readily obtained. As shown in Figure 5, the localized transfer frequencies (F) in both the *E. coli* biofilm and the activated sludge biofilm at the time of the first presence of transconjugants (t = 10 h) are both less than 0.05. While the localized transfer frequency in the activated sludge biofilm gradually increased with time (i.e 0.07 at t = 16 h and ~0.1 at t = 22 h), the transfer frequency in the *E. coli* biofilm rapidly increased to ~0.8 by t = 16 h, followed by a gradual increase to ~0.9 at t = 22 h (Figure 4). These results further illustrated the different transfer mechanisms in these two biofilms as discussed above.

Although the high spatial and temporal information is necessary to study the dynamics of the transfer process, we also noticed that some of microscopic images in the preselected areas did not contain any conjugation events. Therefore, at the end of the assay, tiled images of an enlarged area (~41 mm^2) were acquired to give a global view of the biofilm. As shown in Figure 6a b (an overview) and Figure 6c (an enlarged area), the transconjugant areas in the *E. coli* biofilm are large and close to each other, whereas those in the activated sludge

DOI: 10.1021/acs.est.8b03281
Environ. Sci. Technol. 2018, 52, 11132−11141

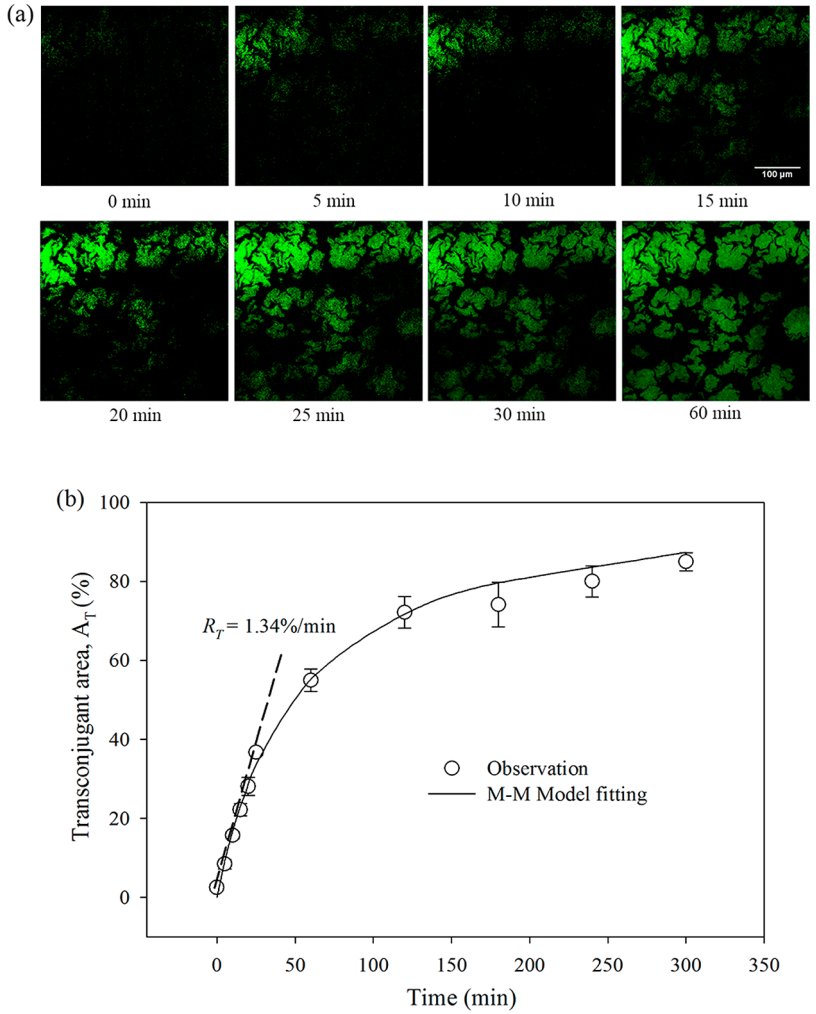

Figure 3. Cascading spread of transconjugants in the *E. coli* biofilm: (a) Representative time-lapse images of one location with conjugation events; (b) The changes of the transconjugant area within an image (A_T%) with time (n = 3, the error bars are SD).

Table 1. Plasmid Transfer Kinetics in *E. coli* and Environmental Community Biofilms

type	variable		unit	*E. coli* biofilm		Activated sludge community biofilm
Donor	species		-	*P. putida* KT 2440		*P. putida* KT 2440
	species		-	*E. coli* ATCC 25922		Activated sludge bacteria
Recipient	max. specific growth rate[a]	μ_m	h^{-1}	0.89		0.71
	duration of data[b]		h	0.4[e]	3[f]	10[g]
Trans-conjugant	localized transfer rate[c]	R_T	$\%{\cdot}h^{-1}$	81 ± 1.2	33 ± 1.5	0.006 ± 0.004
		R^2	-	(0.993−0.997)	(0.921−0.976)	(0.880−0.979)
	specific increment rate[d]	μ_T	h^{-1}	7.5 ± 0.86	2.9 ± 0.89	0.26 ± 0.14
		R^2	-	(0.947−0.965)	(0.875−0.946)	(0.968−0.990)

[a]Calculated from the monolayer colonies on-chip in the initial stage of biofilm. [b]The time span of the data used for calculation. [c]Transfer rate R_T is calculated by linearly fitting the percentage of transconjugants with the experimental time, $R_T = \Delta A_T/\Delta t$. [d]Specific increment rate μ_T is calculated by exponential modeling the increment of transconjugants with time, $\ln(A_T/A_{T_\lambda}) = \mu_T{\cdot}(t\text{-}\lambda)$, λ is the lag time. [e]Data at the first 25 min from t = 10 h, which represents the "explosive" stage of plasmid transfer, from three sites. [f]Data from 10 to 13 h, from eight sites. [g]Data from 8 to 18 h, from five sites.

biofilms are small and scattered. Furthermore, there are much more transconjugant sites in the activated sludge, suggesting more occurrences of the initial conjugation events by the original *P. putida* donor. However, the total area of transconjugants in the activated sludge biofilm only occupies 2.2% of the total scanned area, while that in the *E. coli* biofilm occupies 6.8% at the end of the experiments. These results are in good agreement with the microscopic study, showing that secondary conjugation by transconjugants can play a prominent role in gene dissemination in biofilms.

Diversity Analysis of the Recipient and Transconjugant Community. At the end of the on-chip mating assay, the activated sludge biofilms were collected and FACS sorted to collect the transconjugants (SI Figure S6). The collected transconjugants and the initial recipient cells (i.e., four activated sludge samples, two each from two WWTPs)

DOI: 10.1021/acs.est.8b03281
Environ. Sci. Technol. 2018, 52, 11132−11141

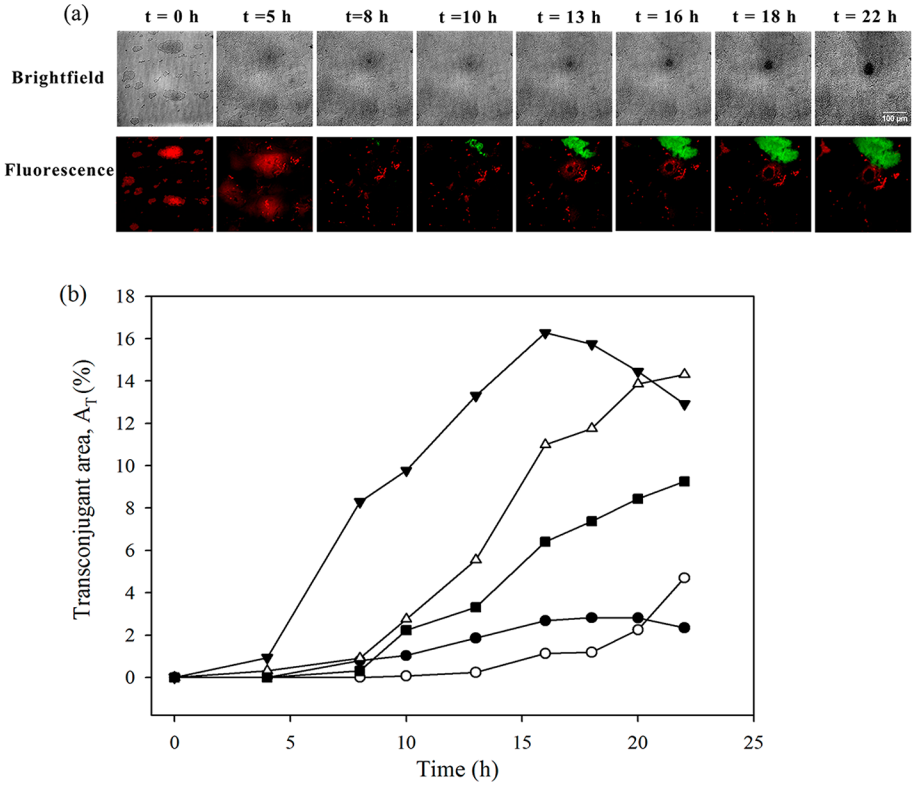

Figure 4. Plasmid transfer process between the *P. putida* KT2440 and the activated sludge community: (a) representative time-lapse images of the bacteria on chip. Note, the activated sludge cells are colorless and trasconjugants emit green fluorescence. (b) The changes of the transconjugant area (A_T%) from five random positions with time. Each curve shows typical characteristics of a bacterial growth curve, including lag-, exponential-, stationary-, and declined phases. Due to different lag time and specific increment rate, not all the phases are presented on each curve within the 22 h experiments.

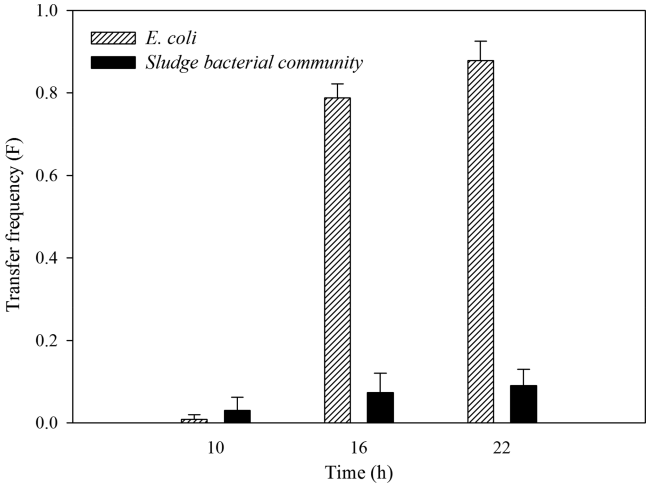

Figure 5. Localized transfer frequency of the plasmid in the *E. coli* biofilm and the activated sludge biofilm at different time points (n = 6, the error bars are SD).

were 16S rDNA amplicon sequencing. The four recipient communities samples (RB) showed similar diversities, which contain 56 operational taxonomic units (OTUs) at 97% similarity for genus level (SI Figure S7). About 46% of these recipient OTUs were detected in the transconjugant pools (TB) (SI Figure S7), illustrating the broad-host-range nature of the plasmid RP4. However, the OTUs composition of the transconjugants was different from the recipient communities both in key genera and in relative abundance (Figure 7). In particular, the presence of a genus in the transconjugant pool was independent of its relative abundance in the recipient community. Taking the genus *Myroides* as an example, its abundance in the transconjugant pool was in a much higher relative percentage than that in the recipient community. This phenomenon corroborates with previous study that OTU abundance in the transconjugant pools could not directly link with their abundance in the soil recipient community, due to the high variability in permissiveness of the broad-range-host plasmid RP4.[11]

It is worth noting that a number of genera in the transconjugant pool are associated with human pathogens, including *Aeromonas*,[29] *Pseudomonas*, and *Enterobacteriaceae*.[11,30] Since most of their related human pathogens have shown resistance to current antibiotics, the permissiveness of these genera to the transfer of the plasmid RP4 should alert us to pay attention on their potential roles in promoting ARG dissemination in the environment.

DISCUSSIONS

Microfluidics Facilitates the Study of the Dynamics of Gene Transfer in Biofilms. Most current experimental methods can only determine the *overall* gene transfer frequency in biofilms, and thus cannot differentiate different transfer mechanisms.[12,31,32] In addition, since these methods depend on bulk culture, they are beset with various unknown conditions in biofilm formation (such as those associated with the biofilm's internal structure), and are therefore restricted in their analytical power when studying gene transfer processes.[12]

DOI: 10.1021/acs.est.8b03281
Environ. Sci. Technol. 2018, 52, 11132−11141

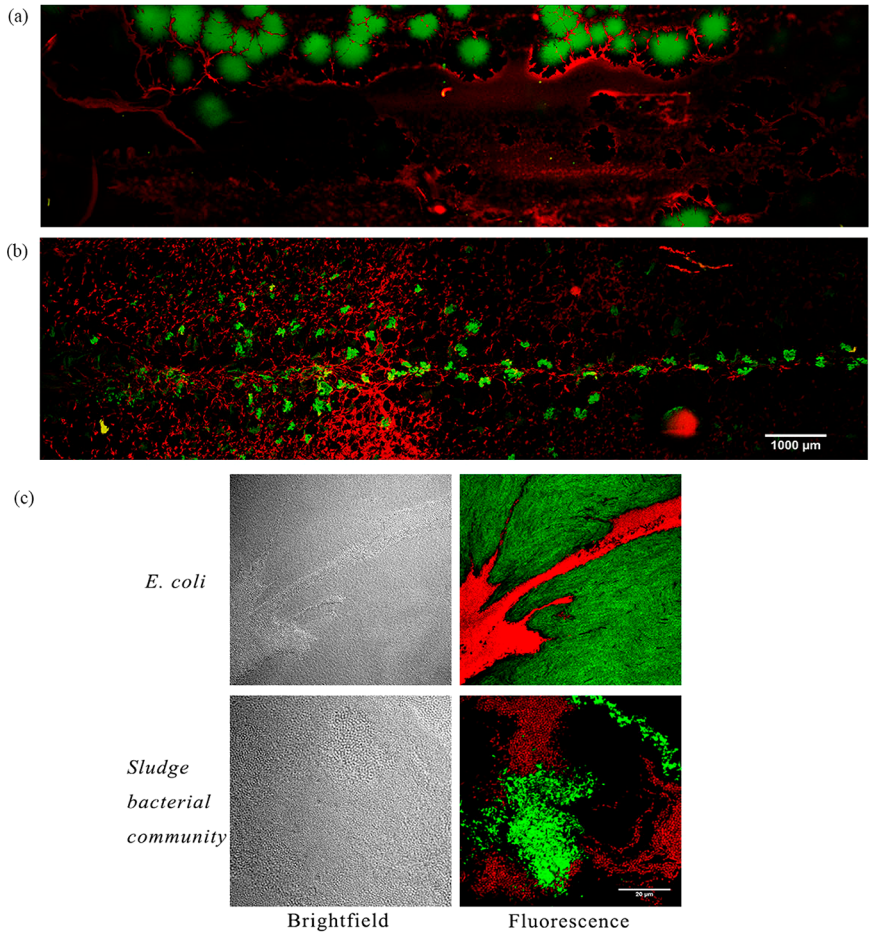

Figure 6. CLSM images of bacteria at the end of the mating assay on chip at 24h: (a) *P. putida* KT2440 and *E. coli* biofilm; (b) *P. putida* KT2440 and the activated sludge microbial community biofilm; (c) Detailed bright-field and fluorescence images of *E. coli* and activated sludge community with *P. putida* KT2440.

The mating assays on the microfluidic device, as described in this study, offer several advantages for the study of gene transfer processes in biofilms. First, in situ formation of a biofilm on chip can be recorded from the on-set of cell seeding. This enables the measurement of cell growth and monitoring of the process of plasmid transfer at the single-cell level with a suitable objective lens (e.g., 100× objective lens, SI Figure S3). Second, exponential growth of cells was maintained by the continuous flow culture. This, together with the physical confinement on chip, facilitates rapid and uniform formation of biofilms as shown in Figures 1 and 4. Furthermore, the use of a thin agarose membrane underneath the flow channel allows the diffusion-driven transport of nutrients. In the early stage of biofilm formation (i.e., monolayer or a few multiple layers of cells), all the cells experienced the same, well-controlled culture regime under the steady nutrient gradients across the chip. This removed potential interference from unknown variations of the culture condition within a biofilm.[33] In the matured stage of a biofilm, cell growth was sustained in a limited thickness (i.e., ∼18 μm in Figure 2 and SI Figure S3) by squeezing bacteria into close contact with each other.[15] As a result, it facilitated the study of the role of structure and composition of biofilms in gene transfer. For the first time, we show that the secondary conjugation by transconjugants can lead to a cascading transfer of the plasmid RP4 in a dense single-strain recipient biofilm.

Structure and Composition of Biofilm Modulate Gene Transfer Routes. The combination of fluorescence protein technology and microfluidics provides a versatile platform for identifying key transfer mechanisms in biofilms of different compositions. As illustrated in Figures 3 and 4, the presence of GFP transconjugants in both biofilms demonstrates successful plasmid-mediated HGT from the *P. putida* KT2440 donor to the potential recipient cells, either a pure *E. coli* strain or a complex activated sludge community. The dynamic tracking of the biofilm formation on chip also allowed the specific increment rate of transconjugant (μ_T) and maximum specific cell growth rate (μ_m) to be determined at the same time. Therefore, the ratio of μ_T to μ_m can serve as a simple indicative of the relative contribution by either HGT or cell division. The substantially high μ_T/μ_m ratio at 8.3 (>5) during the "explosive" spread of transconjugants in the *E. coli* biofilm clearly shows the dominant role of HGT, whereas the low μ_T/μ_m ratio at 0.37 (<0.5) for the activated sludge biofilm suggests an important role of vertical gene transfer in a complex community.

The striking differences between these two biofilms could be due to the opportunity of forming large single-recipient colonies, which is essential for the secondary transfer process. As shown in Figure 1a and 4a, after ∼4 or 5 h of culture, both systems formed close cell-to-cell contacts. Such conditions are known to promote the transfer of the plasmid RP4 due to the

DOI: 10.1021/acs.est.8b03281
Environ. Sci. Technol. 2018, 52, 11132−11141

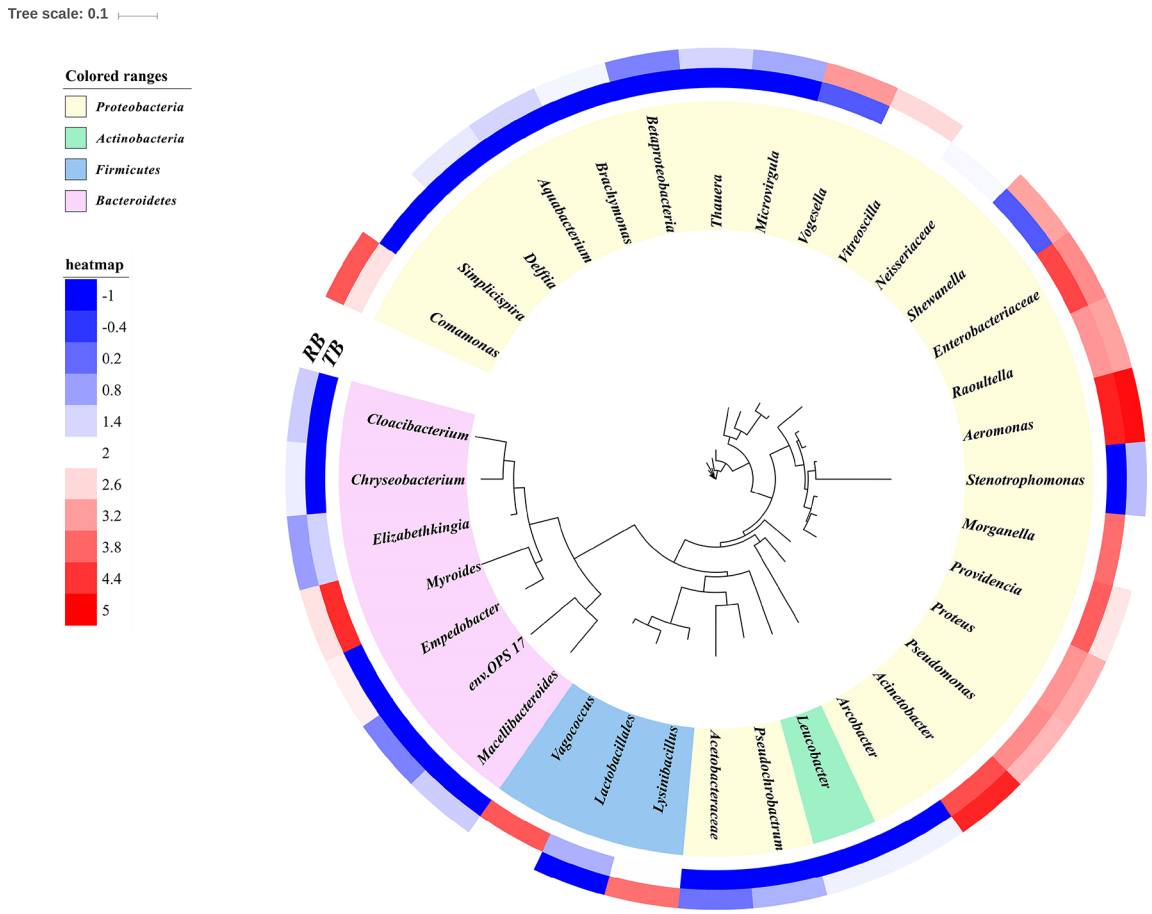

Figure 7. Cladogram showing phylogenetic tree of the genera as well as the heatmap for both the recipient community (RB) and transconjugant pool (TB). The genera are colored according to the phylum they are part of and the values in the heatmap represent the average of the log abundance of each genera in the four RB or TB samples, respectively. Only the top 35 genera were included in the figure.

formation of conjugal pili.[3,34] In the case of genetically identical donors and recipients, conjugation is extremely efficient[9] and fast (e.g., in the range of minutes).[10] However, the frequency of successful HGT decreases exponentially with the phylogenetic distance.[3] Since the activated sludge biofilm only consists of small and randomly scattered donor and recipient colonies, it is highly likely the majority of conjugations are between different species.

Relevance to Antibiotic Resistance and Infection Treatment. As referred to earlier, biofilm formation has been found to be one of the major causes for the failure of conventional antibiotic treatments.[35] Our findings indicate that pure-strain biofilms could lead to a higher risk of treatment failure, particularly in the case of the pathogens associated with the genera found in the transconjugant pool (Figure 7). Currently, many single-species biofilms are frequently found in device-related infections, such as *Staphylococci*, a harmful opportunistic pathogen actively engaged in plasmid-mediated transfer.[36] The surface conditions in these indwelling devices are often similar to those as found on chip in this study, that is, ones which provide rich nutrients and limited space for biofilm formation. Once a few bacterial cells have acquired antibiotic resistance, the scenario of the cascading spread of ARG's across the biofilm might occur.

In terms of biofilms of complex bacterial communities, they exist widely in both persistent/chronic infections[35,37] and in the natural environments.[6] The observed permissiveness of a broad range of genera to the ARG-encoding plasmid RP4 highlighted the fact that plasmid-medicated HGT generally occurs in community type biofilms. Although the activated sludge biofilm studied here did not consist of large single-species colonies and hence no occurrence of cascading spread of the plasmids occurred, the overall transfer frequency was still high (0.05) due to the existence of many plasmid permissive genera. In multiple-species biofilms or in the real-world biofilms where bacteria could move, the scenario for containing both superpermissive species and their large colonies are likely to occur. This could cause severe damage and catastrophic events. Further study of the dynamic process of the ARG transfer in differently structured biofilms can provide valuable insights to develop early prevention and intervention strategies to reduce the likelihood of its occurrence.

■ ASSOCIATED CONTENT

Supporting Information

The Supporting Information is available free of charge on the ACS Publications website at DOI: 10.1021/acs.est.8b03281.

Figure S1: Schematic drawing of the microfluidic device; Figure S2Mating assay of *P. putida* KT2440 and *E. coli* when the PBS flowed through the microfluidics. Figure S3 The bacterial biofilms of *P. putida* KT2440 and activated sludge bacteria community at 24 h: (a) 3D images of biofilm; (b) Z-stack images of different layers

DOI: 10.1021/acs.est.8b03281
Environ. Sci. Technol. 2018, 52, 11132−11141

at a 2 μm internal. Figure S4. The growth curves of *P. putida* KT2440, *E. coli* and the activated sludge bacterial community on the chip; Figure S5. Time-lapse images of other locations with conjugation events of *E. coli* and activated sludge bacterial community (from 10h to 22h); Figure S6. FACS of the biofilms to collect the transconjugants; Figure S7. Microbial diversity of four recipient communities and four transconjugants pools. Protocols for sequence analysis (PDF)

AUTHOR INFORMATION

Corresponding Authors

*(Y.Q.) E-mail: qiuyong@tsinghua.edu.cn.
*(H.Y.) E-mail: huabing.yin@glasgow.ac.uk.

ORCID

Yong Qiu: 0000-0001-5423-6869
Xia Huang: 0000-0003-4076-1464
Huabing Yin: 0000-0001-7693-377X

Notes

The authors declare no competing financial interest.

ACKNOWLEDGMENTS

B.L. acknowledges the support from National Natural Science Foundation of China (51708023) and Fundamental Research Funds for the Central Universities (FRF-TP-16-058A1). Y.Q. acknowledges the support from National Natural Science Foundation of China (51778325). HY acknowledges the support from NERC(NE/P003826/1). The authors thank Dr Cindy Smith for proof-reading, and specially thank Professor Barth F. Smets in Technical University of Denmark for gifting the donor strains.

REFERENCES

(1) Madsen, J. S.; Burmolle, M.; Hansen, L. H.; Sorensen, S. J. The interconnection between biofilm formation and horizontal gene transfer. *FEMS Immunol. Med. Microbiol.* **2012**, *65* (2), 183−95.

(2) Romling, U.; Balsalobre, C. Biofilm infections, their resilience to therapy and innovative treatment strategies. *J. Intern. Med.* **2012**, *272* (6), 541−561.

(3) Soucy, S. M.; Huang, J.; Gogarten, J. P. Horizontal gene transfer: building the web of life. *Nat. Rev. Genet.* **2015**, *16* (8), 472−482.

(4) Sørensen, S. J.; Bailey, M.; Hansen, L. H.; Kroer, N.; Wuertz, S. Studying plasmid horizontal transfer in situ: a critical review. *Nat. Rev. Microbiol.* **2005**, *3* (9), 700−710.

(5) Król, J. E.; Wojtowicz, A. J.; Rogers, L. M.; Heuer, H.; Smalla, K.; Krone, S. M.; Top, E. M. Invasion of E. coli biofilms by antibiotic resistance plasmids. *Plasmid* **2013**, *70* (1), 110−119.

(6) Flemming, H.-C.; Wingender, J.; Szewzyk, U.; Steinberg, P.; Rice, S. A.; Kjelleberg, S. Biofilms: an emergent form of bacterial life. *Nat. Rev. Microbiol.* **2016**, *14* (9), 563−575.

(7) Finley, R. L.; Collignon, P.; Larsson, D. G. J.; McEwen, S. A.; Li, X.-Z.; Gaze, W. H.; Reid-Smith, R.; Timinouni, M.; Graham, D. W.; Topp, E. The Scourge of Antibiotic Resistance: The Important Role of the Environment. *Clin. Infect. Dis.* **2013**, *57* (5), 704−710.

(8) Harrison, E.; Brockhurst, M. A. Plasmid-mediated horizontal gene transfer is a coevolutionary process. *Trends Microbiol.* **2012**, *20* (6), 262−267.

(9) Babi, A.; Lindner, A. B.; Vuli, M.; Stewart, E. J.; Radman, M. Direct Visualization of Horizontal Gene Transfer. *Science* **2008**, *319* (5869), 1533−1536.

(10) Seoane, J.; Yankelevich, T.; Dechesne, A.; Merkey, B.; Sternberg, C.; Smets, B. F. An individual-based approach to explain plasmid invasion in bacterial populations. *FEMS Microbiol. Ecol.* **2011**, *75* (1), 17−27.

(11) Klumper, U.; Riber, L.; Dechesne, A.; Sannazzarro, A.; Hansen, L. H.; Sorensen, S. J.; Smets, B. F. Broad host range plasmids can invade an unexpectedly diverse fraction of a soil bacterial community. *ISME J.* **2015**, *9* (4), 934−945.

(12) Zhong, X.; Droesch, J.; Fox, R.; Top, E. M.; Krone, S. M. On the meaning and estimation of plasmid transfer rates for surface-associated and well-mixed bacterial populations. *J. Theor. Biol.* **2012**, *294*, 144−152.

(13) Jutkina, J.; Rutgersson, C.; Flach, C.-F.; Larsson, D. G. J. An assay for determining minimal concentrations of antibiotics that drive horizontal transfer of resistance. *Sci. Total Environ.* **2016**, *548*, 131−138.

(14) Guo, M.-T.; Yuan, Q.-B.; Yang, J. Distinguishing Effects of Ultraviolet Exposure and Chlorination on the Horizontal Transfer of Antibiotic Resistance Genes in Municipal Wastewater. *Environ. Sci. Technol.* **2015**, *49* (9), 5771−5778.

(15) Li, B.; Qiu, Y.; Glidle, A.; McIlvenna, D.; Luo, Q.; Cooper, J.; Shi, H.-C.; Yin, H. Gradient Microfluidics Enables Rapid Bacterial Growth Inhibition Testing. *Anal. Chem.* **2014**, *86* (6), 3131−3137.

(16) Weibel, D. B.; DiLuzio, W. R.; Whitesides, G. M. Microfabrication meets microbiology. *Nat. Rev. Microbiol.* **2007**, *5* (3), 209−218.

(17) Kou, S.; Cheng, D.; Sun, F.; Hsing, I.-M. Microfluidics and microbial engineering. *Lab Chip* **2016**, *16* (3), 432−446.

(18) Li, B.; Qiu, Y.; Glidle, A.; Cooper, J.; Shi, H.; Yin, H. Single cell growth rate and morphological dynamics revealing an "opportunistic" persistence. *Analyst* **2014**, *139* (13), 3305−3313.

(19) Karimi, A.; Karig, D.; Kumar, A.; Ardekani, A. M. Interplay of physical mechanisms and biofilm processes: review of microfluidic methods. *Lab Chip* **2015**, *15* (1), 23−42.

(20) Kim, J.; Park, H.-D.; Chung, S. Microfluidic Approaches to Bacterial Biofilm Formation. *Molecules* **2012**, *17* (8), 9818−9834.

(21) Yuan, X. F.; Couto, J. M.; Glidle, A.; Song, Y. Q.; Sloan, W.; Yin, H. B. Single-Cell Microfluidics to Study the Effects of Genome Deletion on Bacterial Growth Behavior. *ACS Synth. Biol.* **2017**, *6* (12), 2219−2227.

(22) Musovic, S.; Dechesne, A.; Sorensen, J.; Smets, B. F. Novel Assay To Assess Permissiveness of a Soil Microbial Community toward Receipt of Mobile Genetic Elements. *Appl. Environ. Microbiol.* **2010**, *76* (14), 4813−4818.

(23) Qiu, Y.; Zhang, J.; Li, B.; Wen, X. H.; Liang, P.; Huang, X. A novel microfluidic system enables visualization and analysis of antibiotic resistance gene transfer to activated sludge bacteria in biofilm. *Sci. Total Environ.* **2018**, *642*, 582−590.

(24) Zhang, T.; Yang, Y.; Pruden, A. Effect of temperature on removal of antibiotic resistance genes by anaerobic digestion of activated sludge revealed by metagenomic approach. *Appl. Microbiol. Biotechnol.* **2015**, *99* (18), 7771−7779.

(25) Yang, Y.; Li, B.; Ju, F.; Zhang, T. Exploring Variation of Antibiotic Resistance Genes in Activated Sludge over a Four-Year Period through a Metagenomic Approach. *Environ. Sci. Technol.* **2013**, *47* (18), 10197−10205.

(26) Hong, H.; Ko, H. J.; Choi, I. G.; Park, W. Previously Undescribed Plasmids Recovered from Activated Sludge Confer Tetracycline Resistance and Phenotypic Changes to Acinetobacter oleivorans DR1. *Microb. Ecol.* **2014**, *67* (2), 369−379.

(27) Geisenberger, O.; Ammendola, A.; Christensen, B. B.; Molin, S.; Schleifer, K. H.; Eberl, L. Monitoring the conjugal transfer of plasmid RP4 in activated sludge and in situ identification of the transconjugants. *FEMS Microbiol. Lett.* **1999**, *174* (1), 9−17.

(28) Soda, S.; Otsuki, H.; Inoue, D.; Tsutsui, H.; Sei, K.; Ike, M. Transfer of antibiotic multiresistant plasmid RP4 from *Escherichia coli* to activated sludge bacteria. *J. Biosci. Bioeng.* **2008**, *106* (3), 292−296.

(29) Igbinosa, I. H.; Beshiru, A.; Odjadjare, E. E.; Ateba, C. N.; Igbinosa, E. O. Pathogenic potentials of Aeromonas species isolated from aquaculture and abattoir environments. *Microb. Pathog.* **2017**, *107*, 185−192.

(30) Cai, L.; Zhang, T. Detecting Human Bacterial Pathogens in Wastewater Treatment Plants by a High-Throughput Shotgun

DOI: 10.1021/acs.est.8b03281
Environ. Sci. Technol. 2018, 52, 11132−11141

Sequencing Technique. *Environ. Sci. Technol.* **2013**, *47* (10), 5433−5441.
(31) Simonsen, L.; Gordon, D. M.; Stewart, F. M.; Levin, B. R. Estimating the rate of plasmid transfer-An end point method. *J. Gen. Microbiol.* **1990**, *136* (11), 2319−2325.
(32) Lagido, C.; Wilson, I. J.; Glover, L. A.; Prosser, J. I. A model for bacterial conjugal gene transfer on solid surfaces. *FEMS Microbiol. Ecol.* **2003**, *44* (1), 67−78.
(33) Fox, R. E.; Zhong, X.; Krone, S. M.; Top, E. M. Spatial structure and nutrients promote invasion of IncP-1 plasmids in bacterial populations. *ISME J.* **2008**, *2*, 1024−1039.
(34) Soda, S.; Otsuki, H.; Inoue, D.; Tsutsui, H.; Sei, K.; Ike, M. Transfer of antibiotic multiresistant plasmid RP4 from escherichia coli to activated sludge bacteria. *J. Biosci Bioeng* **2008**, *106* (3), 292−6.
(35) Lebeaux, D.; Ghigo, J. M.; Beloin, C. Biofilm-Related Infections: Bridging the Gap between Clinical Management and Fundamental Aspects of Recalcitrance toward Antibiotics. *Microbiol. Mol. Biol. Rev.* **2014**, *78* (3), 510−543.
(36) Hall-Stoodley, L.; Costerton, J. W.; Stoodley, P. Bacterial biofilms: From the natural environment to infectious diseases. *Nat. Rev. Microbiol.* **2004**, *2* (2), 95−108.
(37) Percival, S. L.; Hill, K. E.; Williams, D. W.; Hooper, S. J.; Thomas, D. W.; Costerton, J. W. A review of the scientific evidence for biofilms in wounds. *Wound Repair Regen.* **2012**, *20* (5), 647−657.

DOI: 10.1021/acs.est.8b03281
Environ. Sci. Technol. 2018, 52, 11132−11141